Decay of the Peroxide Intermediate in Laccase: Reductive Cleavage of the O−O Bond

Amy E. Palmer,‡ Sang Kyu Lee,‡ and Edward I. Solomon*,‡

Contribution from the Department of Chemistry, Stanford University, Stanford, California 94305

Received February 9, 2001

Abstract: Laccase is a multicopper oxidase that contains four Cu ions, one type 1, one type 2, and a coupled binuclear type 3 Cu pair. The type 2 and type 3 centers form a trinuclear Cu cluster that is the active site for O_2 reduction to H_2O. To examine the reaction between the type 2/type 3 trinuclear cluster and dioxygen, the type 1 Cu was removed and replaced with Hg^{2+}, producing the T1Hg derivative. When reduced T1Hg laccase is reacted with dioxygen, a peroxide intermediate (**P**) is formed. The present study examines the kinetics and mechanism of formation and decay of **P** in T1HgLc. The formation of **P** was found to be independent of pH and did not involve a kinetic solvent isotope effect, indicating that no proton is involved in the rate-determining step of formation of **P**. Alternatively, pH and isotope studies on the decay of **P** revealed that a proton enhances the rate of decay by 10-fold at low pH. This process shows an inverse k_H/k_D kinetic solvent isotope effect and involves protonation of a nearby residue that assists in catalysis, rather than direct protonation of the peroxide. Decay of **P** also involves a significant oxygen isotope effect ($k^{16}O_2/k^{18}O_2$) of 1.11 ± 0.05, indicating that reductive cleavage of the O−O bond is the rate-determining step in the decay of **P**. The activation energy for this process was found to be ∼9.0 kcal/mol. The exceptionally slow rate of decay of **P** is explained by the fact that this process involves a $1e^-$ reductive cleavage of the O−O bond and there is a large Franck−Condon barrier associated with this process. Alternatively, the $2e^-$ reductive cleavage of the O−O bond has a much larger driving force which minimizes this barrier and accelerates the rate of this reaction by $\sim 10^7$ in the native enzyme. This large difference in rate for the $2e^-$ versus $1e^-$ process supports a molecular mechanism for multicopper oxidases in which O_2 is reduced to H_2O in two $2e^-$ steps.

Introduction

Laccase (*p*-diphenol:dioxygen oxidoreductase, EC 1.10.3.2) belongs to the family of multicopper oxidases which includes ascorbate oxidase (AO), ceruloplasmin (CEP), FET3p, and bilirubin oxidase.[1] Functionally, all multicopper oxidases couple four one-electron substrate oxidations with the four-electron reduction of dioxygen to water. Spectroscopic studies, sequence alignments, and crystal-structure comparisons reveal that the active site of all multicopper oxidases contains at least four Cu ions.[1−5] These Cu ions are classified into three different types of sites: the type 1 (T1), or blue Cu site, the type 2 (T2), or normal Cu site, and the type 3 (T3), or coupled binuclear Cu site which is comprised of two Cu^{2+} ions antiferromagnetically coupled through a bridging hydroxide.[6] These sites are defined by the spectroscopic properties they exhibit in the oxidized (Cu^{2+}) state. Crystal structures of multicopper oxidases[6,7] confirm spectroscopic results[8,9] showing that the T2 and T3 Cu sites are in close proximity (within 4 Å) and together form a trinuclear Cu cluster. The T1 Cu site is about 13 Å from this trinuclear cluster.

In multicopper oxidases, the T1 Cu site accepts electrons from substrate and transfers the electrons ∼13 Å to the T2/T3 trinuclear Cu cluster which binds and activates O_2 for reduction to H_2O.[1] Most studies on the catalytic cycle have focused on laccase because of its simplicity. Reaction of fully (four-electron) reduced native laccase with O_2 has been shown to produce a transient species which decays ($k = 0.03\ s^{-1}$, 25 °C)[10] to the resting, fully oxidized enzyme. This species is present under turnover conditions, suggesting that it plays a key role in the catalytic cycle.[11] This transient species (often called the native intermediate, **N**) exhibits an $S = {}^1/_2$ EPR signal at <20 K which broadens with $^{17}O_2$, leading to the suggestion that it was an oxygen radical intermediate.[12] Absorption and EPR studies[11−13] on **N** revealed that the T1 and T3 Cu sites are oxidized, and

* To whom correspondence should be addressed.
‡ Department of Chemistry, Stanford University, Stanford CA, 94305.

(1) Solomon, E. I.; Sundaram, U. M.; Machonkin, T. E. *Chem. Rev.* **1996**, *96*, 2563−2605.
(2) Messerschmidt, A. *Multi-Copper Oxidases*; Messerschmidt, A., Ed.; World Scientific Publishing Co.: River Edge, NJ, 1997.
(3) Messerschmidt, A.; Huber, R. *Eur. J. Biochem.* **1990**, *187*, 341−352.
(4) Dooley, D. M.; Rawlings, J.; Dawson, J. H.; Stephens, P. J.; Andréasson, L.-E.; Malmström, B. G.; Gray, H. B. *J. Am. Chem. Soc.* **1979**, *101*, 5038−5046.
(5) Ducros, V.; Brzozowski, A. M.; Wilson, K. S.; Brown, S. H.; Østergaard, P.; Schneider, P.; Yaver, D. S.; Pedersen, A. H.; Davies, G. J. *Nat. Struct. Bio.* **1998**, *5*, 310−316.
(6) Messerschmidt, A.; Ladenstein, R.; Huber, R. *J. Mol. Bio.* **1992**, *224*, 179−205.
(7) Zaitseva, I.; Zaitsev, V.; Card, G.; Moshov, K.; Bax, B.; Ralph, A.; Lindley, P. *J. Biol. Inorg. Chem.* **1996**, *1*, 15−23.
(8) Spira-Solomon, D. J.; Allendorf, M. D.; Solomon, E. I. *J. Am. Chem. Soc.* **1986**, *108*, 5318−5328.
(9) Cole, J. L.; Clark, P. A.; Solomon, E. I. *J. Am. Chem. Soc.* **1990**, *112*, 9534−9548.
(10) Andréasson, L.-E.; Reinhammar, B. *Biochim. Biophys. Acta* **1976**, *445*, 579−597.
(11) Andréasson, L.-E.; Brändén, R.; Reinhammar, B. *Biochim. Biophys. Acta* **1976**, *438*, 370−379.
(12) Aasa, R.; Branden, R.; Deinum, J.; Malmstrom, B. G.; Reinhammar, B.; Vanngard, T. *Biochem. Biophys. Res. Commun.* **1976**, *70*, 1204−1209.
(13) Aasa, R.; Branden, R.; Deinum, J.; Malmstrom, B. G.; Reinhammar, B.; Vanngard, T. *FEBS Lett.* **1976**, *61*, 115−119.

10.1021/ja010365z CCC: $20.00
Published on Web 06/19/2001

therefore at least three electrons have been transferred to the oxygen. Magnetic circular dichroism (MCD) spectroscopy indicated that the $S = {}^1/_2$ paramagnetic species has significant Cu^{2+} character, suggesting that the T2 Cu is also oxidized.[14] Recent results on **N** reveal that all four electrons (one from each Cu) have been transferred to the oxygen, resulting in a fully oxidized trinuclear Cu^{2+} cluster in which all three Cu ions in the trinuclear cluster are bridged by the oxygen product.[15] This structure differs from that of the resting enzyme where the T2 is no longer bridged to the T3 site.

To focus specifically on the reaction of the T2/T3 trinuclear Cu cluster with O_2, a derivative of the enzyme was prepared in which the T1 Cu was removed and replaced by a spectroscopically silent and redox inactive Hg^{2+}.[16−18] This T1HgLc derivative provides two advantages: (1) it permits observation of the spectroscopic features of the trinuclear Cu center unobstructed by the T1 Cu, and (2) it deprives the enzyme of one of the electrons it needs to reduce O_2 to H_2O. The fully (three-electron) reduced T1HgLc was shown to react with O_2 to produce a peroxide-level intermediate (**P**) in which peroxide bridges between the reduced T2 Cu and oxidized T3 Cu.[19] MCD studies of **P** revealed that it decayed via a native intermediate-like species. Initial kinetic studies revealed that the formation of **P** (in T1HgLc) and **N** (in native Lc) was dependent on O_2 concentration and that the second-order rate constants for formation were comparable.[20] Because **N** is further along the O_2-reduction reaction pathway (two electrons further reduced than **P**, vide supra), these results suggested that **P** is kinetically competent to be a precursor to **N**.

The present study examines the mechanism of decay of **P** in T1HgLc. In particular, pH, isotope studies, and temperature dependence on the kinetics of formation and decay were undertaken to gain insight into the mechanism of O−O bond cleavage, its activation energy, and to assess whether these processes involve proton- as well as electron transfer. This study further combines experimental data with modeling to compare the slow rate of decay of **P** in T1HgLc to the analogous fast reaction in the native enzyme. Finally, this leads to a model of the Franck−Condon barrier contribution to the cleavage of the O−O bond and supports a molecular mechanism for the $4e^-$ reduction of O_2 to H_2O which proceeds through two $2e^-$ steps.

Experimental Section

Enzyme Preparation and Characterization. *Rhus vernicifera* laccase (native Lc) was isolated from acetone powder (Saito and Co., Osaka, Japan) according to published procedures.[21,22] Laccase activity was assayed spectrophotometrically using *N*,*N*-dimethyl-*p*-phenylenediamine as a substrate.[21] The T1Hg-substituted derivative (T1HgLc), in which the T1 Cu is removed and replaced by Hg^{2+}, was prepared as described previously.[16−18] Both the native laccase and T1HgLc were characterized by absorption and EPR. UV/visible absorption spectra were recorded on a Hewlett-Packard HP8452A diode array spectrophotometer in either 1, 0.2, or 0.1 cm quartz cuvettes. The protein concentration was determined using the extinction coefficient (ϵ_{280} = 90 000 M^{-1} cm^{-1}) of the absorption band at 280 nm.[23] Copper concentration was determined spectrophotometrically using 2,2′-biquinoline[24] or by atomic absorption spectroscopy. EPR spectra at 77 K were obtained using a liquid nitrogen finger dewar and a Bruker ER 220-D-SRC spectrometer. Spin quantification of protein samples was determined using a Cu standard (1.0 mM $CuSO_4 \cdot 5H_2O$ with 2 mM HCl and 2 M $NaClO_4$ [25]). All chemicals were reagent grade and were used without further purification. Water was purified to a resistivity of 15−18 MΩ cm using a Barnstead Nanopure deionizing system.

Kinetic Studies. Experiments were performed on an Applied Photophysics SX.18MV, Stopped Flow Absorption Spectrophotometer equipped with a Hg/Xe Arc lamp. The system was made anaerobic by outfitting it with PEEK tubing, plungers, and valves and by scrubbing with 5 mM dithionite for about 30 min prior to use. The dithionite was completely removed by washing with anaerobic buffer. The temperature was maintained using a water/ethylene glycol temperature bath (Brinkmann RM6). All experiments were performed at 20 °C and with a path length of 1 cm unless otherwise stated.

For kinetic experiments, the protein solution (native Lc or T1HgLc), sodium dithionite, and buffer were thoroughly deoxygenated and cycled into a Vacuum Atmospheres Nexus-1 anaerobic glovebox. The buffer used was either 100 mM MES, 100 mM potassium phosphate, or 100 mM potassium hydrogen phthalate. A slight excess of electron equivalents of dithionite was added to the protein solution and allowed to react for 45 min. The dithionite was then removed using a microcon concentration device (50 000 MW cutoff, Amicon, Inc.); the protein solution was washed four to five times with deoxygenated buffer and spun at 10 000 rpm using a VWR Scientific model-V micro-centrifuge in the glovebox. The reduced protein was then loaded into a 1 mL gastight Hamilton syringe, cycled out of the glovebox, and transported to the stopped-flow spectrometer. The reduced protein was loaded into one of the spectrometer syringes, and care was taken to prevent O_2 exposure. The other spectrometer syringe was loaded with 1 mL of air-saturated buffer. The concentration of O_2 in the buffer was estimated to be about 0.2 mM at 20 °C.[26] The intermediate was formed by mixing equal volumes (about 75 μL each) of reduced protein and air-saturated buffer. Each experiment yielded about 11−13 separate measurements. The absorbance was monitored at 340 nm for T1HgLc and 364 and 614 nm for native Lc. The absorbance at 280 nm was also measured to provide an accurate protein concentration for each experiment. The final protein concentration was 0.013−0.015 mM, and the final O_2 concentration was ∼0.1 mM.

For pH studies, 100 mM buffer solutions were prepared, and the pH was measured using an Orion 420A pH meter and a three-point standard calibration. MES was used for pH = 4.7, 5.0, 5.15, 5.3; both MES and potassium phosphate were used for pH = 5.5, 5.8, 6.0, and 6.5; and potassium phosphate was used for pH = 7.0, 7.5, and 8.0. At pHs where both buffers were used, there was no difference in the observed rate of formation and decay. A stock solution of concentrated protein (∼1 mM) was diluted in the appropriate buffer prior to dithionite reduction, and this same buffer was used to wash out the dithionite. The pH of the protein solution was then measured inside the glovebox to ensure that the proper pH was maintained.

For proton/deuterium isotope studies, buffers were prepared in either H_2O or D_2O (99.9 atom % D, Aldrich). For deuterated buffers, the pD was taken as the pH meter reading + 0.4.[27] All of the experiments were performed with T1HgLc isolated from the same protein preparation. The concentrated protein stock solution was divided into two parts; half of the solution was exchanged into buffer, pH 6.0, and the other half was exchanged into deuterated buffer, pD 6.0. To assess whether the isotope effect observed at low pH (vide infra) resulted from the

(14) Clark, P. A.; Solomon, E. I. *J. Am. Chem. Soc.* **1992**, *114*, 1108−1110.
(15) Lee, S. K.; Solomon, E. I. **2001**, manuscript in preparation.
(16) Morie-Bebel, M. M.; Morris, M. C.; Menzie, J. L.; McMillin, D. R. *J. Am. Chem. Soc.* **1984**, *106*, 3677−3678.
(17) Morie-Bebel, M. M.; Menzie, J. L.; McMillin, D. R. *Biological and Inorganic Copper Chemistry*; Morie-Bebel, M. M., Menzie, J. L., McMillin, D. R., Eds.; Adenine Press: 1984; Vol. 1, pp 89ff.
(18) Severns, J. C.; McMillin, D. R. *Biochemistry* **1990**, *29*, 8592−8597.
(19) Shin, W.; Sundaram, U. M.; Cole, J. L.; Zhang, H. H.; Hedman, B.; Hodgson, K. O.; Solomon, E. I. *J. Am. Chem. Soc.* **1996**, *118*, 3202−3215.
(20) Cole, J. L.; Ballou, B. P.; Solomon, E. I. *J. Am. Chem. Soc.* **1991**, *113*, 8544−8546.
(21) Reinhammar, B. *Biochim. Biophys. Acta* **1970**, *205*, 35−47.
(22) Reinhammar, B. R. M. *Biochim. Biophys. Acta* **1972**, *275*, 245−259.
(23) Meadows, K. A.; Morie-Bebel, M. M.; McMillin, D. R. *J. Inorg. Biochem.* **1991**, *41*, 253−260.
(24) Felsenfeld, G. *Arch. Biochem. Biophys.* **1960**, *87*, 247−251.
(25) Carithers, R. P.; Palmer, G. *J. Biol. Chem.* **1981**, *256*, 7967−7976.
(26) *CRC Handbook of Chemistry and Physics*; CRC Press: Boca Raton, 1986; Vol. 67.

difference in viscosity between H_2O and D_2O (1.005 vs 1.25),[27,28] glycerol was added to the protein solution and to the air-saturated buffer (MES, pH 4.7). Addition of glycerol had no effect on the reaction rate of formation and decay of the intermediate, indicating that the observed rate difference was not due to a viscosity effect.

The $^{16/18}O_2$ isotope studies were performed as described above, with the following modifications. All of the $^{16/18}O_2$ experiments were performed in 100 mM potassium hydrogen phthalate buffer, pH 4.6. The intermediate was formed by mixing equal volumes of reduced protein with O_2-saturated buffer rather than air-saturated buffer. The concentration of O_2 in the buffer was estimated to be about 1.0 mM.[26] The O_2-saturated buffer was prepared in the following way: a syringe was filled with $^{16}O_2$ from a gas cylinder or $^{18}O_2$ from a 1 L bulb (96% $^{18}O_2$, ICON Stable Isotopes), and the syringe was emptied into a solution of deoxygenated buffer. This was performed three times.

The rate of decay as a function of temperature was monitored from $T = 4.2-25$ °C in 100 mM potassium hydrogen phthalate, pH 4.8, and from $T = 20-39.5$ °C in 100 mM potassium phosphate, pH 7.5.

Calculation of Equilibrium Isotope Effects. The equilibrium isotope effect (EIE) can be expressed as a product of three terms: the zero-point energy (ZPE), excited vibrational states (EXC), and the mass and moments of inertia (MMI).[29] These individual contributions to EIE can be calculated using the vibrational frequencies of relevant normal modes (those impacted by isotopic substitution) in the reactant and product. The following expressions[30] are used to calculate the ZPE, EXC, and MMI:

$$\mathrm{ZPE} = \exp\left(\frac{h}{2kT}\left[\sum_i^{3n-6}[(\nu_{16(r)})_i - (\nu_{18(r)})_i] - \sum_i^{3n-6}[(\nu_{16(p)})_i - (\nu_{18(p)})_i]\right]\right)$$

$$\mathrm{EXC} = \prod_i^{3n-6} \frac{1-\exp\left[-\frac{h}{kT}(\upsilon_{16(r)})_i\right]}{1-\exp\left[-\frac{h}{kT}(\upsilon_{18(r)})_i\right]} \prod_i^{3n-6} \frac{1-\exp\left[-\frac{h}{kT}(\upsilon_{18(p)})_i\right]}{1-\exp\left[-\frac{h}{kT}(\upsilon_{16(p)})_i\right]}$$

$$\mathrm{MMI} = \prod_i^{3n-6} \frac{(\upsilon_{18(r)})_i}{(\upsilon_{16(r)})_i} \prod_i^{3n-6} \frac{(\upsilon_{16(p)})_i}{(\upsilon_{18(p)})_i}$$

where h is Planck's constant (6.626×10^{-34} J s), k is Boltzmann's constant (1.38066×10^{-23} J K^{-1}), and T the absolute temperature ($T = 293$ K for the calculations in this paper). The vibrational frequencies for the models used in this paper were taken from experimental data on a number of Cu−oxygen model complexes and are given in Table S1 of Supporting Information along with relevant references.

Calculation of Potential Energy Surfaces. The potential energy (U) surfaces were calculated according to the standard Morse equation, where the reactant is given by $U = D(1 + e^{-2\beta y} - 2e^{-\beta y})$, and the product is approximated as the repulsive part of the reactant curve, $U = D(e^{-2\beta y})$.[31] In these equations, $\beta = \nu_o(2\pi^2\mu/D)^{1/2}$, where ν_o is the vibration frequency of the bond, y is the distortion from the equilibrium bond length, and D is the bond dissociation energy. For the calculations presented in this paper, ν_o was taken as the experimentally determined ν_{O-O} (892 cm^{-1}) for a $Cu_2(OOH)$ model complex,[32] μ was set at 8 g/mol, and D was estimated to be between 34 and 50 kcal/mol, based on experimental values and theoretical predictions for peroxide.[33−35] To account for the Coulombic repulsion between the two negatively charged (q) product fragments of the $2e^-$ reductive cleavage case, the correction $332\Sigma\{q_1q_2/(r_{12}\epsilon_{eff})\}$ was used with a protein dielectric (ϵ_{eff}) of 15.[36]

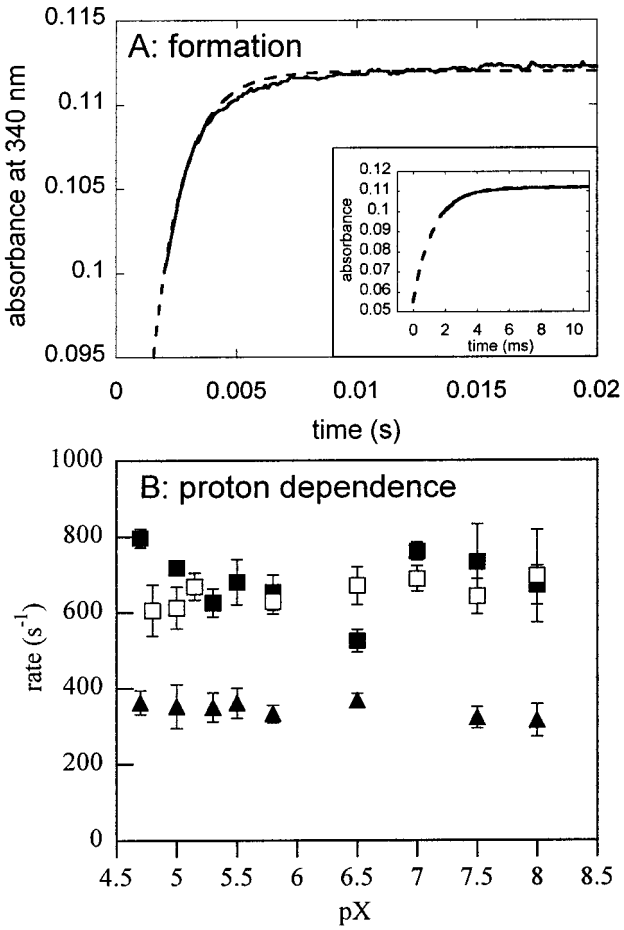

Figure 1. (A) Representative absorption trace (solid line) for the formation of **P** at 340 nm. The data were fit to a single exponential (dashed line), and the rate constant was extracted. The inset shows the complete curve fit. For all experiments $A_{initial}$ ranged from 0.04 to 0.06.[37] (B) The rate of formation of **P** (squares) and **N** (triangles) as a function of pX, where X = H (closed symbols) or D (open symbols). Each data point represents the average rate obtained from 8−15 different absorption traces, taken from at least two different experiments.

Results and Analysis

Formation Kinetics. It was previously shown that the reaction of reduced T1HgLc with O_2 leads to a peroxide-level intermediate with absorption features at 340, 470, and 710 nm.[19] To determine whether formation of this peroxide intermediate (**P**) was proton-dependent, stopped flow absorption spectroscopy was used to measure the rate of formation of **P** as a function of pH and pD. The rate of formation was obtained by monitoring the absorbance at 340 nm as a function of time. Figure 1A displays a representative absorption trace (solid line) obtained at pH = 4.7. The data can be fit (dashed line) to a single exponential ($y = A_{initial} + \Delta A(1 - e^{-kx})$) and the rate constant (k) can be extracted. The inset to Figure 1A shows the full curve

(27) Schowen, K. B. *Solvent Hydrogen Isotope Effects*; Schowen, K. B., Ed.; Plenum Press: New York, 1978; pp 225−283.
(28) Karsten, W. E.; Lai, C.-J.; Cook, P. F. *J. Am. Chem. Soc.* **1995**, *117*, 5914−5918.
(29) Melander, L.; Saunders Jr., W. H. *Reaction Rates of Isotopic Molecules*; John Wiley and Sons: New York, 1980.
(30) Tian, G.; Klinman, J. P. *J. Am. Chem. Soc.* **1993**, *115*, 8891−8897.
(31) Savéant, J.-M. *Dissociative Electron Transfer*; Savéant, J.-M., Ed.; JAI Press Inc.: New York,1994; Vol. 4, pp 53−116.
(32) Root, D. E.; Mahroof-Tahir, M.; Karlin, K. D.; Solomon, E. I. *Inorg. Chem.* **1998**, *37*, 4838−4848.
(33) Baldwin, A. C. *Thermochemistry of Peroxides*; Baldwin, A. C., Ed.; John Wiley and Sons: New York, 1983; pp 97−104.
(34) Luo, X.; Flemming, P. R.; Rizzo, T. R. *J. Chem. Phys.* **1992**, *96*, 5659−5667.
(35) Bach, R. D.; Ayala, P. Y.; Sclegel, H. B. *J. Am. Chem. Soc.* **1996**, *118*, 12758−12765.
(36) Warshel, A.; Papazyan, A.; Muegge, I. *J. Biol. Inorg. Chem.* **1997**, *2*, 143−157.

fit where $A_{initial}$ is ~0.05, and the dead time of the instrument is 2 ms.[37] Figure 1B presents the rate of formation as a function of pX (where X = H or D for experiments performed in H_2O or D_2O, respectively). The dark squares represent the rates obtained in protonated buffer and the open squares represent the rates obtained in deuterated buffer. As is evident from Figure 1B, the rate of formation of **P** was independent of pH and did not display a kinetic solvent isotope effect. This indicates that a proton is not involved in the rate-determining step of formation of **P**.

In analogous experiments, we also examined the rate of formation of the native intermediate (**N**) in native Lc, which is further along the O_2-reduction reaction pathway, as a function of pH. The data were obtained my monitoring the abs at 364 nm and are represented by the dark triangles in Figure 1B. The rate of formation of **N** was also found to be independent of pH, indicating that a proton is not involved in the rate-determining step of formation of **N**. It is important to note that at all pH's **N** and **P** have comparable rates of formation indicating that **P** is kinetically competent to be a precursor to **N**. This is consistent with earlier studies which examined the rate of formation of **P** and **N** at a single pH.[20]

We examined whether there was a kinetic oxygen isotope effect on the formation of **P** by mixing reduced T1HgLc with buffer saturated with $^{16}O_2$ or $^{18}O_2$. However, most of **P** was formed in the dead time of the instrument (Figure S1, Supporting Information) and we could not accurately assess whether there was a difference between $^{16}O_2$ and $^{18}O_2$. A lower limit for the rate constant is $>1500\ s^{-1}$. The rate of formation of **P** is faster when a higher O_2 concentration is used; this is consistent with earlier studies that showed formation to be dependent on O_2.[20]

Decay Kinetics. (1) Proton Dependence. Stopped flow absorption spectroscopy was also used to examine the rate of decay of **P**. The absorbance at 340 nm was measured as a function of time and the data could be fit to a single exponential ($y = A_{initial} - \Delta A(1 - e^{-kx})$). A sample absorption trace (solid line) and fit (dashed line) for decay of **P** at pH 4.7 are shown in Figure 2A. Figure 2B displays the rate of decay of **P** as a function of pH (triangles) and pD (circles). The rate of decay is clearly dependent on pH and the sigmoidal behavior is indicative of a single protonation equilibrium. The rate of decay at low pH is 10-fold faster than the rate of decay at high pH (0.003 vs 0.0003 s^{-1}), and the pK_a of the protonatable group is 5.8. These data are consistent with previous studies on the pH dependence of decay, but the rates obtained are slightly different because in the present experiments dithionite was removed (vide infra).[19] The inset in Figure 2B displays the model that best fit the experimental data. This model yields the following expression[38] for the experimental rate (k_{obs}):

$$k_{obs} = \frac{k_2[H^+] + k_1K_a}{K_a + [H^+]}$$

where k_1 is the rate of decay at high pH and k_2 is the rate of decay at low pH.[39] A model involving an initial protonation equilibrium followed by decay of the protonated species was considered but did not fit the high pH data.

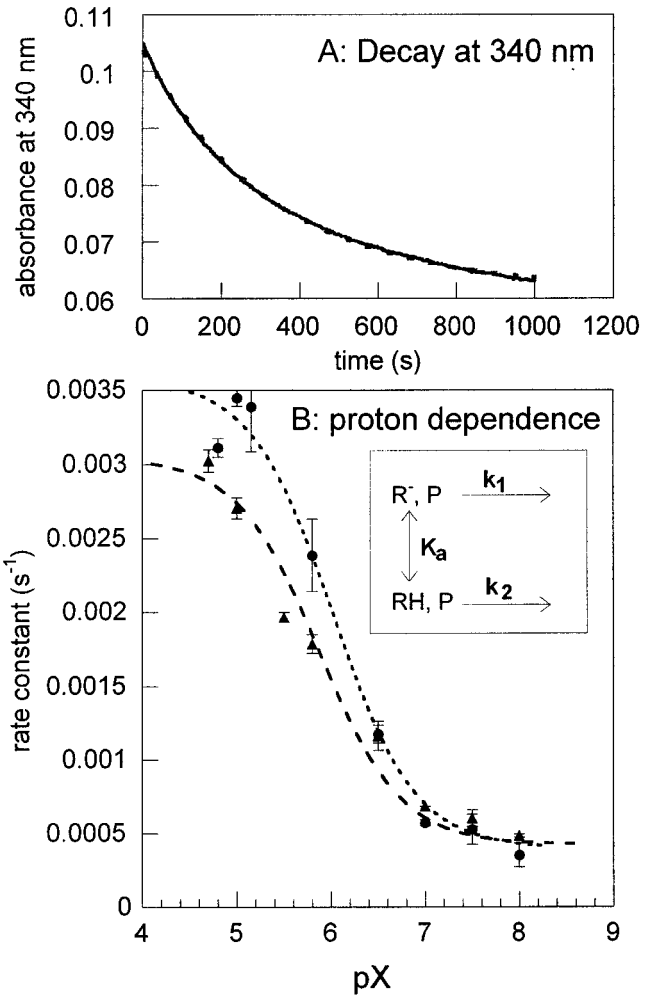

Figure 2. (A) Sample absorption trace (solid line) for the decay of **P** at 340 nm. The data were fit to a single exponential (dashed line) and the rate constant was extracted. (B) Rate of decay of **P** as a function of pH (triangles) and pD (circles). The pH and pD data were fit (dashed and dotted line, respectively) according to the equation $k_{obs} = (k_2[H^+] + k_1K_a)/(K_a + [H^+])$ which was derived from the model depicted in the inset of (B).

Previous studies suggested that the protonatable species might be a nearby residue, but no structural comparison of the intermediate at high and low pH was available. Figure 3 shows the absorption spectrum of **P** at low pH (dashed line, pH 4.7) and high pH (solid line, pH 7.5).[40] The spectra are quite similar. If the equilibrium discussed above involved protonation of **P**, the peroxide to T3 Cu charge transfer (CT) transitions (340 and 470 nm bands, indicated by the arrows) would be significantly affected. The additional bonding interaction between the proton and peroxide would be expected to increase the CT energy by ~5000 cm^{-1} (by lowering the energy of the peroxide donor orbital) and decrease the CT intensity by ~1/3 (by increasing the e^- affinity and decreasing the charge donation of the peroxide).[32,41] The strong similarity between the spectrum of **P** at low and high pH, in particular the identical energies of the peroxide to Cu CT transitions, confirms that the protonation equilibrium does not involve direct protonation of **P**, and further implicates a nearby species.

(37) For the fully reduced protein, the absorbance should be around 0.02. Our data were consistently fit with an initial absorbance of 0.04−0.06 due to a small amount of protein oxidation.

(38) Fersht, A. *Enzyme Structure and Mechanism*, 2nd ed.; W. H. Freeman and Co.: New York, 1985.

(39) This expression is different from eq 3 in ref 19. Equation 3 contained an error; the rate increase at low pH was 30-fold (not 10^6 fold).

(40) It should be noted that in ref 19, the intermediate was compared to the oxidized rather than the reduced spectrum, and so the$\Delta\epsilon$ was reported to be 3500 $M^{-1}\ cm^{-1}$. The ϵ340 of the intermediate is the same in both studies.

(41) Solomon, E. I.; Tuczek, F.; Root, D. E.; Brown, C. A. *Chem. Rev.* **1994**, *94*, 827−856.

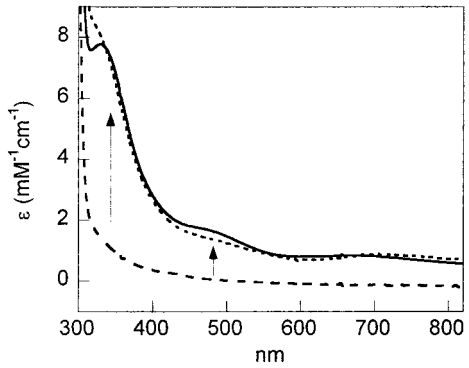

Figure 3. Absorption spectra of **P** at pH 7.5 (solid line), pH 4.7 (dotted line), and reduced T1HgLc (dashed line). Spectra were recorded on an HP 8452 UV/Visible Spectrometer. The low pH spectrum was scaled by 1.16 to account for the amount of intermediate which had decayed at the time the spectrum was taken (60 s). The actual ϵ_{340} was 6.39 $mM^{-1}cm^{-1}$ which is what would be expected if ~20% of the intermediate had decayed (according to $k \approx 0.003$ s^{-1} at pH 4.7).

The rate of decay of **P** as a function of pD is shown in Figure 2B (circles). The data are fit with the same expression outlined above. At low pH, an inverse kinetic solvent isotope effect (k_H/k_D) of 0.89 is observed, while at high pH no isotope effect is observed ($k_H/k_D \approx 1$).[42] Therefore, at low pH a proton assists in the decay whereas at high pH, no proton is involved.

The observation of an inverse isotope effect in enzyme catalyzed reactions has often been attributed to medium effects, viscosity effects, acid dissociation of a thiol, or dissociation of a metal-chelated water.[28,43] It is straightforward to rule out the first three of these possibilities. The sharp sigmoidal curve of Figure 2b is consistent with a single protonatable species and argues against medium effects. [44,45] The viscosity effect was tested by adding glycerol (25% v/v) to the H_2O reaction solutions at low pH; the rate of decay did not change. Finally, the pK_a of the proton involved in decay of **P** is significantly lower than would be expected for a Cys-SH (p$K_a \approx 8-9$).[46]

There is a water molecule bound to the T2 Cu in resting, fully oxidized laccase with a pK_a between 6 and 7.[47] Because this water molecule is released at some point in the catalytic cycle,[48] its dissociation upon decay of **P** could explain the inverse isotope effect observed at low pH. However, the T2-bound H_2O has a reported p$K_a \approx 6-7$ in the oxidized enzyme and this would have to *decrease* to ~5.8 in **P**. In **P**, the T2 Cu is reduced and this decrease in oxidation state from fully oxidized laccase would be expected to *increase* the pK_a of the T2-bound H_2O. Therefore, it seems the pK_a of the group involved in the decay of **P** argues against involvement of the T2-bound H_2O.

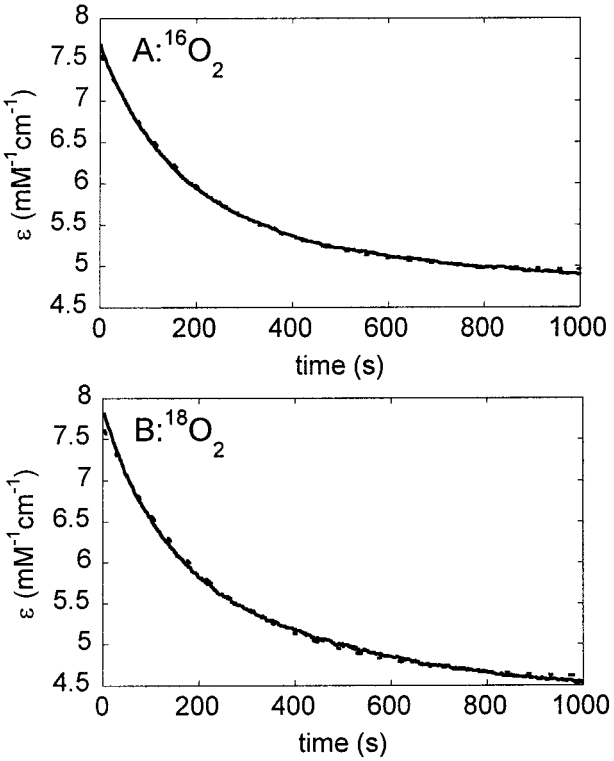

Figure 4. Representative absorption traces for the decay of P (A) $^{16}O_2$ and (B) $^{18}O_2$. Data (solid line) were fit (dashed line) to a single exponential.

It was previously suggested that a carboxylic acid (Asp73 in AO) could donate a proton as **P** decays.[19] While ionization of a carboxylic acid does not typically yield inverse isotope effects, it would be possible if bonding to the proton of interest is stronger in the transition state (higher force constant, steeper potential energy surface) than in the reactant.[49] Because the decay of **P** involves cleavage of the O−O bond (vide infra), an unstable oxide species would be produced along the reaction coordinate and this species could be stabilized by protonation, thus forming a strong OH bond. A carboxylic acid would have a pK_a in the right range and therefore could be the species that donates a proton as **P** decays.

(2) Oxygen Isotope Effect. P was prepared by mixing reduced T1HgLc with buffer saturated with either $^{16}O_2$ or $^{18}O_2$ and the rate of decay was monitored by stopped flow absorption spectroscopy. Measurement of the rate of decay was repeated 6 times. Representative data and fits for $^{16}O_2$ and $^{18}O_2$ are presented in Figure 4a and b (respectively). The full set of data and rates are given in Figure S2 and S3 of Supporting Information. The rate of decay of **P** at pH 4.6 and $T = 20$ °C was 0.00465 ± 0.00007 s^{-1} when the intermediate was prepared with $^{16}O_2$ and 0.00416 ± 0.00019 s^{-1} when prepared with $^{18}O_2$.[50] This yields a kinetic oxygen isotope effect ($k^{16}O_2/k^{18}O_2$) of 1.11 ± 0.05.

(42) If all variables are allowed to float in the fitting of the pH and pD profiles, the fits predict a small normal isotope effect of ~2 at high pH. To test this effect, we measured the rate of decay at pH and pD = 8.0 and T = 33.4 °C (where the rate of decay is faster and differences would be more obvious). No difference in the rate of decay could be detected, indicating that there is no isotope effect at high pH. In the fits presented in Figure 2, the rate of decay at high pH was fixed at 0.0004 s^{-1}, and the remaining variables were allowed to float. The R value decreases from 0.9917 to 0.9852 for the pH fit and 0.995 to 0.9944 for the pD fit.

(43) Quinn, D. M.; Sutton, L. D. *Theoretical Basis and Mechanistic Utility of Solvent Isotope Effects*; Quinn, D. M., Sutton, L. D., Eds.; CRC Press: Boca Raton, pp 73−126.

(44) Medium effects generally result from a large number of protons involved in hydrogen bonding or electrostatic interactions, each of which contributes a small isotope effect.

(45) Schowen, K. B.; Schowen, R. L. *Solvent Isotope Effects on Enzyme Systems*; Schowen, K. B., Schowen, R. L., Eds.; Academic Press: New York, 1982; Vol. 87, pp 551−607.

(46) Holm, R. H.; Kennepohl, P.; Solomon, E. I. *Chem. Rev.* **1996**, *96*, 2239−2314.

(47) Tamilarsan, R.; McMillin, D. R. *Biochem. J.* **1989**, *263*, 425−429.

(48) $^{17}O_2$ isotope studies have shown that the water, which is bound to the T2 Cu, derives from molecular oxygen and is released upon turnover.

(49) Klinman, J. P. *Adv. Enzymol.* **1978**, *46*, 415−494.

(50) It should be noted that these rates are slightly higher than the rates obtained in the pH studies as the samples were run in two different buffers. We found that the rate of decay in potassium hydrogen phthalate buffer was consistently slightly higher than in MES buffer. The abs and EPR spectrum of the intermediate and the resting trinuclear cluster are unaffected by the different buffers, and therefore this effect could be due to a slight change in the redox potential of the T2 Cu.

Table 1. Calculation of Equilibrium Isotope Effects[a]

		ZPE	EXC	MMI	EIE
1	$Cu_2OOH \leftrightarrow Cu_2 + {}^{-}OOH$	1.094	1.060	0.886	1.029
2	$Cu_2OOH \leftrightarrow Cu_2 + H_2O_2$	1.056	1.060	0.891	0.999
3	$Cu_2OOH \leftrightarrow Cu_2O + {}^{\bullet}OH$	1.146	1.046	0.893	1.072
4	$Cu_2OOCu \leftrightarrow 2 \times Cu_2O$	1.108	1.047	0.922	1.070
5	$H_2O_2 \leftrightarrow {}^{\bullet}OH + {}^{\bullet}OH$	1.138	1.004	0.939	1.074

[a] See Experimental section for explanation of calculations and Table S1 in supporting Information for frequencies used in calculations. ZPE = zero point energy, EXC = excited vibrational states, MMI = mass and moments of inertia.

The kinetic isotope effect (KIE) for a reaction involving a change in bond order can be related to the equilibrium isotope effect (EIE) for complete loss of the bond defining the reaction coordinate. This is expressed as:

$$k_{16}/k_{18} = (K_{16}/K_{18})^x$$

where x can vary from 0 to 1. If x is close to 0 then the transition state resembles the reactant and if x is close to 1 then the transition state resembles the product.[49] Thus, the EIE provides an upper limit on the value of the KIE for complete loss of the bond defining the reaction coordinate. This method has been utilized by Burger et al. to gain insight into the mechanism of decay of activated bleomycin.[51] As outlined in the Experimental Section, the EIE for a reaction can be calculated using vibrational data for the reactant and product.

It is evident from absorption spectroscopy that decay of **P** results in loss of the 340 and 470 nm absorption bands (peroxide π^*_σ and π^*_v to Cu^{2+} CT transitions, respectively).[19] Table 1 presents the calculated EIE for a number of different model reactions that could account for loss of the peroxide to Cu^{2+} CT transitions. Reactions 1 and 2 involve dissociation of peroxide from a Cu dimer. In reaction 1, which has an EIE of ~1.029, no new bonds are formed, and a hydroperoxide anion simply dissociates from the Cu. In Reaction 2, which would be expected to exhibit a slightly lower EIE of ~0.999, a new O−H bond is formed, and as the peroxide dissociates from the Cu, H_2O_2 is generated. The EIEs for these reactions are lower than the experimental KIE, indicating that decay of **P** does not involve simple dissociation of peroxide.

The intensity of the peroxide to Cu^{2+} CT transitions would also decrease if the O−O bond were cleaved upon decay of **P**. Reactions 3 and 4 represent two different scenarios involving cleavage of the O−O bond. Spectroscopic studies have lead to possible structural models for **P**, where the peroxide either binds externally as a μ-1,1-hydroperoxide bridging between the T2 and one of the T3 Cu ions, or internally bridges all three Cu ions in the trinuclear cluster (vide infra).[19,52] Reaction 3 addresses the first structural model and involves cleavage of the O−O bond in a Cu dimer bridged by a μ-1,1-hydroperoxide. In this reaction, as the O−O bond is cleaved, part of the product ($^{\bullet}$OH) would be released into solution while the other fragment would remain bound to the Cu. Reaction 3 yields an isotope effect of ~1.072, within the range of the experimental value. Reaction 4 addresses the other structural model in which the peroxide is bound internally to all three Cu centers in the trinuclear cluster. Upon O−O bond cleavage, both the oxygen atoms would remain bound to Cu in the product. This type of reaction would be expected to yield an EIE of ~1.07, also within the experimentally observed value. Finally, reaction 5 represents homolytic cleavage of the O−O bond in H_2O_2 and is included for comparison to reactions 3 and 4. As can be seen in Table 1, reaction 5 yields an EIE ~1.074, which is very similar to the values obtained for cleavage of the O−O bond when peroxide is bound to Cu. The large kinetic oxygen isotope effect observed upon decay of **P** reveals that there is a significant change in O−O bond order and indicates that in the rate-determining step, the O−O bond is cleaved.

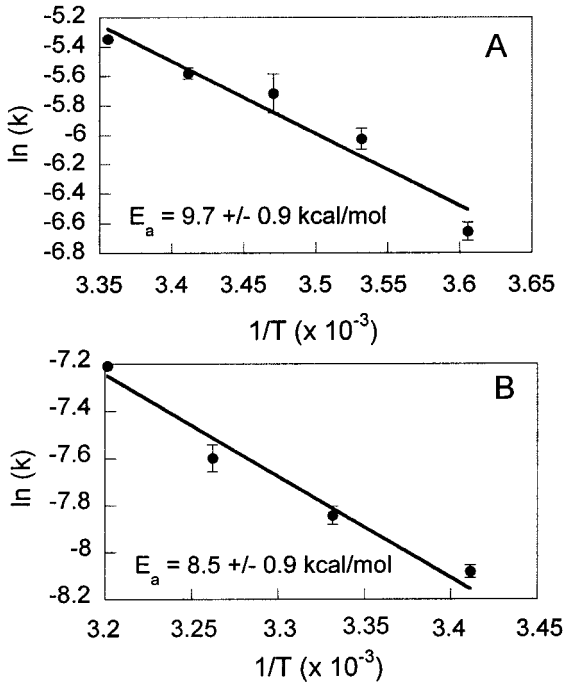

Figure 5. Temperature dependence of decay of **P** at pH 4.8 (A) and pH 8.0 (B). The data were fit to $k = A\ e^{-E_a/RT}$. The fit was varied to determine the standard deviation for the value of E_a obtained.

(3) Temperature-Dependent Arrhenius Behavior. Figure 5 shows the rate of decay of **P** as a function of temperature at pH 4.8 (5A) and pH 7.5 (5B).[53] The data were fit to the Arrhenius equation, $k = A\ e^{-E_a/RT}$, where a plot of ln(k) versus $1/T$ yields a slope equal to $-E_a/R$. The experimentally determined activation energy was the same within experimental error at low pH and high pH (9.7 ± 0.9 kcal/mol and 8.5 ± 0.9 kcal/mol, respectively).

(4) Excess Reductant. Previous studies on **P** utilized two different methods to reduce T1Hg laccase prior to reaction with O_2.[19] The first method involved anaerobic dialysis of T1Hg laccase with excess dithionite followed by anaerobic dialysis against buffer to remove dithionite from the protein solution. The second method involved stoichiometric reduction of T1Hg laccase with dithionite and any excess dithionite and oxidized dithionite products were not removed from the protein solution. In this earlier work it was noted that **P** decayed ~10x faster when it was prepared from T1Hg laccase reduced by the later method (k_{obs} = 0.0012 s^{-1} vs 0.0002 s^{-1} at pH 7.4). In the present study, the impact of dithionite on the rate of decay of **P** was tested more systematically by preparing two different reduced T1Hg laccase solutions. In both solutions, T1Hg laccase

(51) Burger, R.; Tian, G.; Drlica, K. *J. Am. Chem. Soc.* **1995**, *117*, 1167−1168.

(52) Sundaram, U. M.; Zhang, H. H.; Hedman, B.; Hodgson, K. O.; Solomon, E. I. *J. Am. Chem. Soc.* **1997**, *119*, 12525−12540.

(53) Potassium hydrogen phthalate buffer was used for pH 4.8, and potassium phosphate was used for pH 7.5. As noted above, phthalate buffer yielded slightly higher rates than MES or phosphate buffer. The temperature dependence was also performed in potassium phosphate buffer at pH 4.8, and this yielded slightly lower rates but the same slope, and therefore the same activation energy.

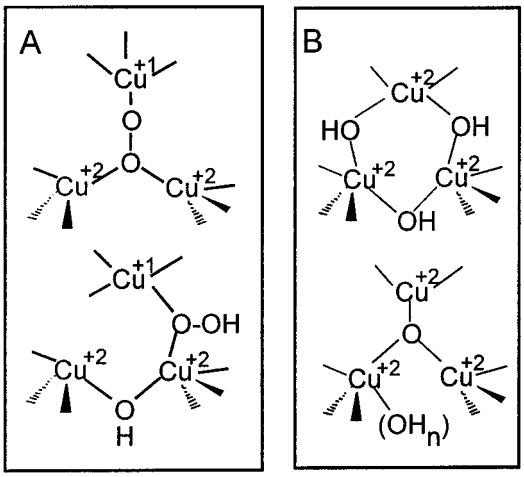

Figure 6. Spectroscopically defined structural models for **P**(A) and **N** (B). In each model, the T2 Cu is on top, and the T3 Cu ions are on the bottom. In **P**, the T2 Cu contains two His ligands and a water ligand, while each of the T3 Cu ions contains three His ligands. In **N**, the T2 Cu contains two His ligands, and each of T3 Cu ions contains three His ligands.

was reduced with a slight excess of dithionite, but in one case the dithionite was washed out before the reduced protein was reacted with O_2 and in the other case it was not. When dithionite was not removed, the decay of **P** exhibited biphasic kinetics where the initial fast phase was about 10x faster than the slower phase ($k_{obs} = 0.003$ s^{-1} vs 0.0004 s^{-1} at pH = 5.5, $T = 4.4$ °C). In the case where dithionite was removed, **P** decayed with $k_{obs} = 0.0005$ s^{-1}, similar to the slow phase observed above.

The above results do not indicate whether excess dithionite or the presence of oxidized dithionite product was responsible for increasing the rate of decay of **P**. EPR spin-trapping studies using 5,5-Dimethyl-1-pyrroline-*N*-oxide (DMPO) were initially pursued in an effort to detect whether •OH was produced upon decay of **P**. Although no DMPO−OH adducts were detected,[54] the DMPO did trap a radical species and yielded an adduct with $A^N = 14.5$ G and $A^{\beta H} = 16.3$ G (Figure S2, Supporting Information). This signal is characteristic of $SO_3^{-\bullet}$ bound to DMPO.[55] Sulfur oxy anions and oxy radicals undergo numerous reactions in solution, and $SO_3^{-\bullet}$ likely derives from oxidized dithionite.[56] This study suggests that in addition to excess reduced dithionite, radical products of oxidized dithionite are present and could accelerate the decay of **P**. These results indicate that if extra electrons are readily available, the rate of decay of the intermediate is greatly increased.

Discussion

Earlier studies on the reaction of reduced T1HgLc with O_2 identified the presence of an oxygen intermediate[20] and employed a variety of spectroscopic techniques to characterize the structure of this intermediate.[19] It was determined that this species involves peroxide bridging between the reduced T2 Cu and oxidized T3 Cu site.[19,52] These earlier studies also suggested that this peroxide intermediate (**P**) decayed to the resting enzyme through a native intermediate-like (**N**) species. Figure 6 shows possible structural models for **P**[19,52] and **N**[15] which were developed from spectroscopic data. These models suggest that the O−O bond is broken in the formation of **N** from **P**. In the present study, the large kinetic oxygen isotope effect ($k^{16}O_2/k^{18}O_2$) of 1.11 ± 0.05 observed upon decay of **P** experimentally establishes that this process involves cleavage of the O−O bond and demonstrates that bond cleavage is the rate-limiting step. Spectroscopic studies on **P** have shown that the reduced T2 Cu in the intermediate is oxidized to Cu^{2+} upon its decay (Supporting Information, Figure S5).[19] The rate of T2 Cu oxidation to the cupric state by EPR parallels the rate of decay of **P**, indicating that decay of **P** involves 1e$^-$ electron transfer from the T2 Cu. We have now shown that decay of **P** also involves cleavage of the O−O bond, and therefore this process is a 1e$^-$ reductive cleavage (an electron is transferred to the peroxide and the bond is cleaved). The temperature dependence of decay reveals that the activation energy for this process is ∼9 kcal/mol. These results provide insight into the mechanism of 1e$^-$ O−O bond cleavage in T1 Hg laccase as well as the general mechanism of the 4e$^-$ reduction of O_2 to H_2O in the native enzyme.

Proton Involvement. The pH and proton/deuterium studies indicate that while a proton assists in the decay of **P** at low pH, no proton is involved at high pH. Absorption spectroscopy revealed that the protonation equilibrium did not affect the electronic structure of **P** and therefore argues against direct protonation of the intermediate. The observed pH dependence and inverse isotope effect are consistent with a model in which a nearby carboxylic acid is implicated as the protonatable species. It is important to note that the intermediate still decays at high pH, that is, in the absence of the stabilizing proton. This suggests that decay does not involve a coupled proton and electron transfer (i.e. a single chemical step), but rather proton transfer after the electron has been transferred and the O−O bond has begun to cleave.

One-Electron Reductive Cleavage of the O−O Bond. Decay of **P** is exceptionally slow (0.003 s^{-1} at low pH and 0.0003 s^{-1} at high pH). To understand why this process is so slow, we previously considered the factors that govern electron transfer: electronic coupling matrix element (H_{DA}), driving force ($\Delta G°$), and reorganization energy (λ). We suggested that because $\Delta G° \approx 0$ for a 1e$^-$ transfer from the T2 Cu to peroxide, there would be a large barrier for this process.[19,57] We now have detailed information on the decay of **P**, in particular we know that the O−O bond is cleaved in the rate-determining step, and we know the experimental activation energy for this process.

Our experimental E_a can be compared to the E_a predicted from a model which describes decay as involving concerted electron transfer and bond breaking. Savéant and co-workers have studied dissociative electron transfer (i.e., reductive cleavage) in alkyl halides.[31,58,59] Similar to Marcus−Hush theory for electron transfer, the activation free energy ($\Delta G^‡$) is a quadratic function of the free energy ($\Delta G°$) and is given by the

(54) It should be noted that if •OH were produced, it would more likely react indiscriminately with the protein than diffuse out of the active site to react with the spin trap.[67] Numerous studies[68,69] have shown that •OH can react rapidly with amino acid side chains and the peptide backbone where the resulting heterogeneous protein radical is undetected by EPR.

(55) Mottley, C.; Mason, R. P.; Chignell, C. F.; Sivarajah, K.; Eling, T. E. *J. Biol. Chem.* **1982**, *257*, 5050−5055.

(56) Hayon, E.; Treinin, A.; Wilf, J. *J. Am. Chem. Soc.* **1972**, *94*, 47−57.

(57) The driving force can be estimated by comparing the redox potential ($E°$) of the T2 Cu (0.37 V)[22] to the general redox potential for the one electron reduction of peroxide ($E°$ for $H_2O_2 + H^+ + e^- \rightarrow \bullet OH + H_2O$ of 0.38 V).[70] Thus, there is essentially no driving force ($\Delta G° \approx 0$) for a one-electron transfer from the T2 Cu to peroxide.

(58) Andrieux, C. P.; Savéant, J.-M.; Tardy, C. *J. Am. Chem. Soc.* **1998**, *120*, 4167−4175.

(59) This model uses Morse curves to approximate the energy of the bond to be cleaved in the reactant and the two fragments formed in the product, where the product is modeled as the repulsive part of the reactant curve. This approximation is based on the assumption that the repulsive term results from the interaction of core electrons and therefore should not be significantly affected by additional valence electrons.

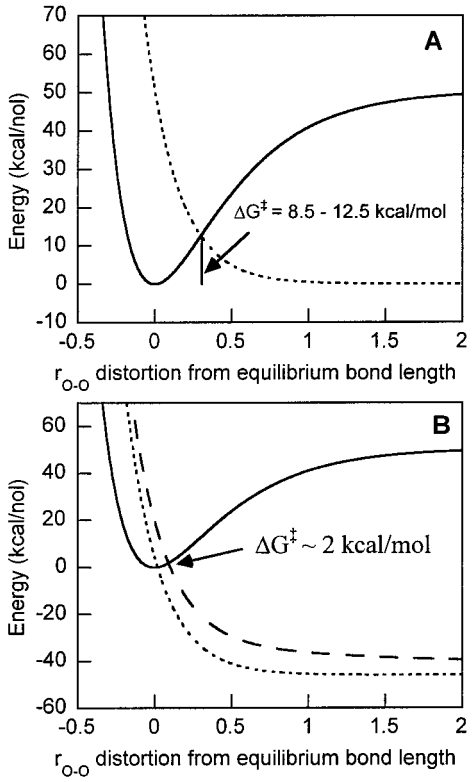

Figure 7. Morse potential energy surfaces for the 1e$^-$ (A) and 2e$^-$ (B) reductive cleavage of peroxide. The equations and parameters used to create the surfaces are presented in the Experimental Section.

following expression:

$$\Delta G^{\ddagger} = \left(\frac{D + \lambda_o}{4}\right)\left(1 + \frac{\Delta G^{\circ}}{D + \lambda_o}\right)^2$$

As is evident from this expression, if $\lambda_o \ll$ D and ΔG° is zero, the contribution from the bond breaking to the activation energy is $^1/_4$ the bond dissociation energy (D).

In predicting the E_a for 1e$^-$ cleavage of peroxide, if we assume that $\lambda_o \ll D$,[31] $\Delta G^\circ \approx 0$, and use the parameters given in the Experimental Section, the potential energy surfaces depicted in Figure 7A are obtained. The range in possible values of D (34−50 kcal/mol),[33−35] leads to an activation energy ($\sim D/4$) of 8.5−12.5 kcal/mol. While this model only accounts for the contribution of O−O cleavage to the E_a and does not include contributions from other bonds that are undoubtedly altered upon decay, it does predict an activation energy in the range of what is observed experimentally for the decay of **P** (9 kcal/mol).[60] This model helps provide insight into the slow decay of **P** in T1HgLc. Because the T1 Cu has been replaced by Hg^{2+}, only three electrons are readily available to reduce O_2. The first two electrons come from the T3 Cu site and are transferred to the O_2 to form **P** and only one electron (from the T2 Cu) is readily available for further reduction.[61] As the analysis above suggests, the 1e$^-$ reductive cleavage of an O−O bond has a significant Franck−Condon barrier and would be a slow process.

It is important to note that if **P** decays by a 1e$^-$ reductive cleavage of the O−O bond, to form **N**, either $^\bullet$OH must be released into solution, or an extra electron must be obtained from somewhere else in the protein or solution. In the present study, we found that if excess dithionite was added, **P** decayed more rapidly, indicating that a second electron readily accelerates the decay process.

Two-Electron Reductive Cleavage of the O−O Bond: Molecular Mechanism of laccase. While **P** has been isolated, and is in fact quite stable in T1HgLc for the reasons discussed above, it has not been detected in the native enzyme. However, there are two experimental results that suggest **P** is relevant to the mechanism of O_2 reduction in the native enzyme. The first was the observation that in T1HgLc **P** decays via **N**.[19] The second was the similarity in the rate of formation of **P** (in T1HgLc) and **N** (in native Lc), indicating that **P** is kinetically competent to be a precursor to **N**.[20,62] These data suggest that both T1HgLc and the native enzyme proceed by the same general reaction mechanism: $E_{red} + O_2 \rightarrow \mathbf{P} \rightarrow \mathbf{N} \rightarrow E_{ox}$. If this is the case, then in the native enzyme $\mathbf{P} \rightarrow \mathbf{N}$ must be much faster than in T1HgLc and therefore no buildup of **P** is observed. Given the experimental rate of formation of **P** and **N**, kinetic modeling can be used to estimate a lower limit for the $\mathbf{P} \rightarrow \mathbf{N}$ step in the native enzyme, assuming that a build-up of ~10% **P** would be within the limits of experimental detection. Using these constraints, a lower limit of ~350 s^{-1} is obtained. This can be compared to the rate for the $\mathbf{P} \rightarrow \mathbf{N}$ step in T1HgLc (0.0003 s^{-1}) and it is evident that in the native enzyme this step would be $>10^6$-times faster.

In the native enzyme, both the T1 and the T2 Cu sites would be reduced in **P**, and therefore two electrons would be available for reductive cleavage of the O−O bond. The model used above can be applied to the 2e$^-$ cleavage of the O−O bond to compare the activation energy to that of the 1e$^-$ process. Assuming $\lambda_o \ll D$,[31] and $\Delta G^\circ \approx 1.0$ V (~46 kcal/mol, for $n = 2$ in the Nernst equation)[63] we obtain the potential energy surfaces depicted in Figure 7B. The dotted curve represents the standard repulsive part of the reactant curve while the dashed curve has an additional term added to account for the Coulombic repulsion between the two negatively charged OH^- product fragments.

The curves in Figure 7B show that the 2e$^-$ reductive cleavage of peroxide would have a very low activation energy ($\Delta G^{\ddagger} =$ 0.07−2 kcal/mol); much smaller than that predicted and observed for the 1e$^-$ case because the large driving force for the two-electron process helps to overcome the Franck−Condon barrier. Comparison of the activation barrier ($\Delta G^{\ddagger}$) predicted for the 2e$^-$ case to that for the 1e$^-$ case, gives an estimated 10^7-fold difference in reaction rate, which is in agreement with the experimental difference of $>10^6$. This model suggests that **P** is not detected in the native enzyme because the $\mathbf{P} \rightarrow \mathbf{N}$ reaction in the native enzyme involves the 2e$^-$ rather than 1e$^-$reductive cleavage of peroxide.

The above analysis provides insight into the molecular mechanism of O_2 reduction in the multicopper oxidases in which the 4e$^-$ reduction proceeds by two 2e$^-$ steps (Figure 8). In general, if reductive cleavage of an O−O bond is an isoenergetic

(60) The Morse potential model presented in Figure 7 makes a number of assumptions; in particular, it neglects contributions to the driving force from the binding of O_2^{2-} and the decay products to Cu and the reorganization energy contributions of these bonds to the decay process. While it is likely that the E° of O−O and the T2 Cu will change upon binding, it is reasonable to assume that the reactant and product would be similarly affected and therefore the ΔG° would not be significantly altered. Assuming that O−O breaking is the only contribution to λ is certainly a simplification. However, much of the additional reorganization would likely occur after the rate-determining step. This is consistent with the fact that the model reproduces the experimentally determined activation energy.

(61) XAS edges studies did not detect any Cu^{3+} in P or N.

(62) The present study examined the formation of **P** and **N** at a number of pHs and found that the pH dependence of formation was the same for **P** and **N** and at all pHs **P** is kinetically competent to be a precursor to **N**

(63) The T1 and T2 Cu sites have similar redox potentials (0.39 and 0.37 V).[22] The driving force can be estimated from the difference of these potentials and the potential for the 2e$^-$ cleavage of peroxide (E° of $H_2O_2 + 2H^+ + 2e- \rightarrow 2\ H_2O$ is 1.37 V).[70]

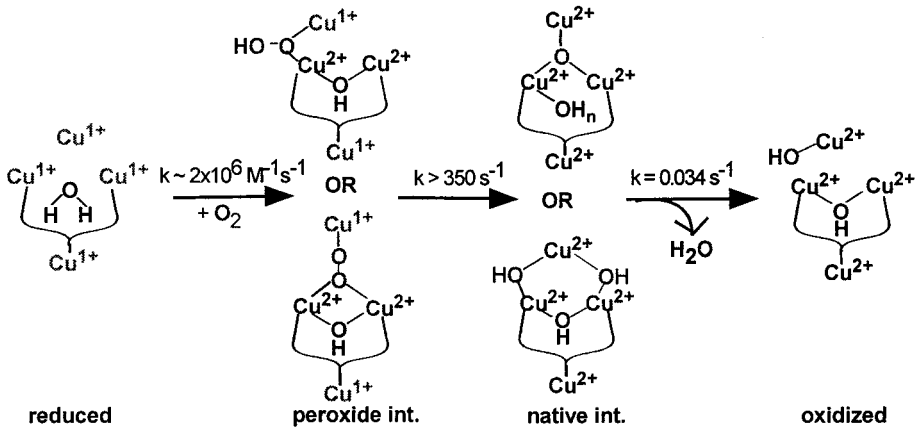

Figure 8. Molecular mechanism for the 4e$^-$ reduction of O_2 to H_2O by the multicopper oxidases. Reduction of O_2 occurs in two 2e$^-$ steps. The second-order rate constant for formation of P was obtained at pH 7.4 and 3 °C.[20] The lower limit on the conversion of **P** to **N** was estimated from rate data at pH 7.5 and 20 °C. The rate of decay of the native intermediate was determined at pH 7.4 and 25 °C.[11]

process, this reaction will be slow due to the large Franck−Condon barrier. However, this reaction can be accelerated either by creating a more stable metal−oxo product (and thereby lowering the barrier)[64] or by coupling two electron transfers (and thereby increasing the driving force).

Summary. In the present study, we have experimentally shown that the decay of **P** involves reductive cleavage of the O−O bond and that this O−O bond cleavage is the rate-determining step. In addition, we have determined that the activation energy for this process is ~9 kcal/mol which is consistent with a model involving the 1e$^-$ reductive cleavage of peroxide. The slow rate of this reaction can be explained by the large Franck−Condon barrier for O−O bond cleavage. In the native enzyme, the reaction of **P** → **N** involves a 2e$^-$ reductive cleavage of the O−O bond which would be ~10^7-times faster than the 1e$^-$ process because the large driving force helps to overcome the Franck−Condon barrier for this reaction.

Acknowledgment. This research was supported by NIH Grant DK31450. A.E.P. is a Franklin Veatch Memorial Fellow.

Supporting Information Available: Table of models and vibrational data used to calculate EIE, absorption trace of P formation as a function of $^{16}O_2$ and $^{18}O_2$, absorption traces and rates of P decay as a function of $^{16}O_2$ and $^{18}O_2$, EPR spectrum of DMPO−SO_3^- adduct, and rate of T2 Cu oxidation upon decay of P (PDF). This material is available free of charge via the Internet at http://pubs.acs.org.

JA010365Z

(64) Lehnert, N.; Ho, R. Y. M.; Que Jr., L.; Solomon, E. I. submitted, **2001**.
(65) Karlin, K. D.; Ghosh, P.; Cruse, R. W.; Farooq, A.; Gultneh, Y.; Jacobson, R. J.; Blackburn, N. J.; Strange, R. W.; Zubieta, J. *J. Am. Chem. Soc.* **1988**, *110*, 6769−6780.
(66) Ling, J.; Farooq, A.; Karlin, K. D.; Loehr, T. M.; Sanders-Loehr, J. *Inorg. Chem.* **1992**, *31*, 2552−2556.
(67) Lerch, K. *Copper Monoxygenases: Tyrosinase and Dopamine β-Monooxygenase*; Lerch, K., Ed.; Marcel Dekker: New York, 1981; Vol. 13, pp 143−186.
(68) Garrison, W. M. *Chem. Rev.* **1987**, *87*, 381−398.
(69) Stadtman, E. R. *Ann. Rev. Biochem.* **1993**, *32*, 797−821.
(70) Sawyer, D. T. *Oxygen Chemistry*; Oxford University Press: New York, 1991.